

A NEW PEACH PALM FIBER MAT FOR POLYURETHANE MATRIX COMPOSITES: BEHAVIOR TO UV-ACCELERATED WEATHERING

MARINA ZAMBONATO FARINA,^{*} KETLIN CRISTINE BATISTA MANCINELLI,^{**}
ANA PAULA TESTA PEZZIN^{*} and DENISE ABATTI KASPER SILVA^{*}

^{*}*Programa de Pós-Graduação em Engenharia de Processos, Universidade de Joinville (Univille), 89219-710 Joinville, Brasil*

^{**}*Programa de Pós-Graduação em Saúde e Meio Ambiente, Universidade de Joinville, 89219-710 Joinville, Brasil*

✉ Corresponding author: D. Abatti Kasper Silva, denise.abatti@univille.br

Received December 13, 2021

Fibers from agricultural residues originating from harvesting heart-of-palm, a renewable resource, have been explored to produce composites with low cost and sustainability, from widely available raw materials. This work investigated the influence of fiber mat percentage and UV-accelerated aging on the properties of polyurethane (PU) matrix composites. The highlight is on the dissociation process of extracting the fibrils from peach palm leaves and producing a fiber mat. The hemicelluloses, cellulose, and lignin contents were determined before and after the dissociation. The mats were incorporated into the matrix by the hand lay-up method corresponding to 6 or 10 wt%. The composites were subjected to accelerated weathering for 90 days and then were characterized by TGA, SEM and tensile testing. The main results indicated that the thermal stability of the composites remained similar to that of neat PU, and the UV-weathering effect on mechanical properties was evident after 90 days of exposure.

Keywords: agribusiness waste, natural fiber, cellulose fibrils, moldable composite, UV-aging

INTRODUCTION

The trend towards environmentally sustainable and biodegradable materials has led researchers to develop new materials, such as polymeric composites with natural fibers, instead of synthetic ones.^{1,2} Moreover, using natural fibers in composites enhances the thermal behavior of the material.³ Examples of natural plant fibers include flax, bamboo, sisal, hemp, ramie, jute, and wood, which have already been used in composites preparation.⁴ As a result, natural fiber polymer based composites are commonly encountered in various applications, such as in the automotive, aircraft, construction, packaging, furniture, textiles, mats, paper and pulp industries.⁵⁻⁹ They represent a cheap and environmentally friendly alternative to petroleum-based materials.¹⁰ The mechanical performance of these composites depends on the fiber and the matrix, as well as on their interfacial adhesion, fiber orientation, manufacturing process, and porosity. There are studies aiming to increase the mechanical

performance of these materials and extend their applications.^{11,12}

Natural plant fibers are composed of cellulose, hemicelluloses, lignin, pectin, waxes, and water-soluble substances.⁵ The hydrophilic nature of these fibers and the impurities present on their surface hinder interfacial adhesion with polymer matrices and lead to composites with poor mechanical properties.¹³ To solve this problem, surface modification methods are necessary,^{1,14} and one strategy is to use compatibilizing agents to improve the compatibility and dispersibility of cellulosic fiber in the matrix.¹³ Another relevant point about natural fibers is their distinct mechanical properties due to their cell wall structure, morphology, and composition. For example, the cellulose content strongly affects fiber stiffness.¹⁵

Fibers from agricultural residues can be used in composites as they have high strength, low cost, high availability and sustainability. In this context, sugarcane bagasse, oil palm, coconut,¹⁶

cornhusk, groundnut shell, cotton,¹⁷ and rice husk fibers¹⁸ have been studied as reinforcements in different matrices. Moreover, their exploitation is in line with one of the 12 principles of green chemistry, *i.e.* using renewable raw materials.¹⁹

The lignocellulosic agricultural residue from peach palm trees (*Bactris gasipaes* HBK) has been studied as filler in polymeric composites.²⁰⁻²⁴ The relevance of this specific residue relies on the cultivation of peach palm, as the extraction of palm hearts generates a large amount of waste. An estimate suggests that less than 10% of the biomass is commercialized as the edible part, with most of the plant remaining on the soil after extraction.²⁵ Additionally, the cultivation of peach palm is a relevant economic activity in some countries, such as Brazil and Costa Rica.²⁴ Just Brazil is responsible for approximately 95% of all palm hearts consumed in the world, the palm heart sector has an estimated annual turnover of US\$ 350 million, generating 8,000 direct and 25,000 indirect jobs, and most of them are in family farms.²⁶ In the light of these, it is essential to search for alternative solutions to the problem of disposal of these residues and for ways to valorize them for sustainable development.

Some efforts have been made to find new applications for this natural fiber waste, including in the development of material composites.²⁰⁻²⁴ An example is the peach palm tree fiber used as a reinforcing filler of a biodegradable matrix based on poly(butylene adipate-co-terephthalate) (PBAT) to develop new green composites for food packaging applications.²⁴ It suggests that peach palm residues in composites may be an alternative to the residue disposal issue.

As regards polyurethane (PU) matrices, a study on the thermal and mechanical properties of castor oil polyurethane/banana fiber composites, as a function of fiber volume, length and alkaline treatment, permitted concluding that the tensile strength and Young's modulus of the composites increased with increasing the fiber volume fraction and the length of the untreated and treated banana fiber.²⁷ Furthermore, the treated banana fiber composites displayed higher tensile strength and elasticity modulus values than the untreated fiber composites due to the morphological and chemical changes in the treated fiber surfaces, promoting better adhesion between the fibers and the polyurethane matrix.

PUs are used in various commercial and technical applications due to their high tensile strength, chemical resistance, good processability

and good mechanical properties.²⁸ Due to the range of chemistries employed in their synthesis, PUs can have many structures (thermoplastic, elastomeric, thermoset, linear and crosslinked PUs).²⁹ Despite their advantages, a particular disadvantage of PU-based materials is their extreme sensitivity to light, particularly UV light,³⁰ which causes deterioration of their physical and mechanical properties,²⁹ triggering their degradation.

In order to propose a new way to use peach palm residue and develop a composite based on sustainability principles, this work presents the development of a material produced with castor oil PU and a peach palm fiber mat. Once produced, the effect of 90 days of UV-aging on the thermal and mechanical properties of the composite material was analyzed, not to mention the effects on its morphology. For this, a dissociated fiber mat production process was developed, and this fiber mat was used as a structure for the PU matrix. Preliminarily, an investigation into the chemical composition of peach palm fibers (PPF) before and after dissociation took place.

EXPERIMENTAL

Materials

The polyurethane resin (PUR) used in this work (trade name: Resin PU Vegetal Type R) was provided by Sinergia Service Ltd. (São Paulo, Brazil). The prepolymer was synthesized from 4,4'-diphenylmethane di-isocyanate (MDI) and prepolymerized with a castor oil-derived polyol. The densities of the prepolymer and the polyol were close to 1.22 and 0.96 g/cm³, respectively. The peach palm leaves were donated by a farmer from a local palm heart cooperative. These leaves were selected, manually divided into strips, and scraped. The botanical name of these strips is the central leaf segment vein. In this work, PPF will be used to denote them.

Methods

Dissociation of fibers and fabrication of mats

After separating and cleaning PPF, the fibers were immersed into a glacial acetic acid:hydrogen peroxide (50:50 v/v) solution at 60 °C for 40 h. This condition was previously defined, and it permitted to identify that the length of peach palm fibers is around 1.0 mm.³¹ After that, the vegetal material was vacuum filtered, washed with running water to remove acid excess, resulting in the pulp. The fiber pulp was homogeneously spread on a screen and dried in an air circulating oven at 40 °C for 30 h to remove excess moisture. This pulp was then passed through a roller

system, forming a fiber mat (Fig. 1). Sheets were formed with 0.3 mm and 0.4 mm thickness, which corresponded to the two mat contents later used in the composites. These mats were then dried at 60 °C to constant mass.

Characterization of plant fiber

Both samples, PPF and the dissociated one, were crushed in a blender, weighed and placed in an oven at 60 °C for 24 h. The hemicelluloses, lignin, cellulose, and ash contents were determined following the methodology described by Silva (1981),³² using triplicate measurements and the mean values (three replicates), expressed as percentages on dry mass. The determination of the moisture was based on fresh material as a parameter. The procedure was to weigh 1 g of the sample on clean, dry watch glasses and then put it in an oven at 105 °C for 30 min, followed by one h in the oven until subsequent weighing. This procedure was repeated until constant mass. One gram of the sample was stirred in 40 mL of distilled water for 30 min at room temperature, filtered, and this procedure was repeated until constant pH. The apparent density of the plant samples was determined using a helium pycnometer (Multivolume 1305 Micromerit Pycnometer). The initial temperature was (24.5 ± 0.3) °C, and there were ten purges in all tests. For morphological analysis, a piece of the mat was coated with gold on Baltec 5CD 050 equipment for 90 s before being observed and photographed on a Zeiss DSM 940A scanning electron microscope (SEM).

Thermogravimetric analysis (TGA) took place on a TA Instruments Q50 device. Five milligrams of samples were heated from 25 to 600 °C, with a heating rate of 10 °C min⁻¹ under an inert atmosphere (N₂).

Polyurethane (PU) and composites preparation

As recommended by the supplier, both components of PU, the prepolymer (component A) and castor oil-derived polyol (component B), in a ratio of 1:1.5 (w/w), were manually mixed for about 8 min, avoiding bubble formation. Then, the solution was poured into a 300 x 180 mm steel mold with 4 mm of thickness and placed in a vacuum oven (under 200 mmHg) for one h at (23 ± 2) °C. Knowing the mass of each fiber mat, a certain mass of PU components was used to produce the PU resin and then the composites. According to the hand lay-up technique, the resin matrix was applied on the mat with the aid of a brush (Fig. 2). After laminating each layer, the material was kept in a vacuum oven (200 mmHg) for two h at room temperature (23 ± 2) °C for pre-curing. The total curing of the composite occurred within three weeks at the same temperature. The nomenclature of the samples is adopted based on the tensile test, using the letter "T" and the following number corresponding to the mass percentage of plant material in the PU matrix, namely 6 wt% (T6) or 10 wt% (T10). For the samples subjected to accelerated weathering, the letter "t" is added to indicate the exposure time, where t₀ = time zero; t₃₀ = 30 days; t₆₀ = 60 days; t₉₀ = 90 days.

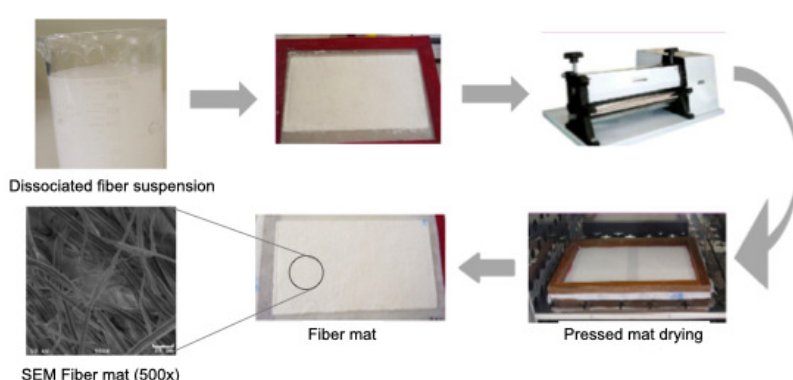


Figure 1: Fiber mat production process and SEM micrograph of the fiber mat

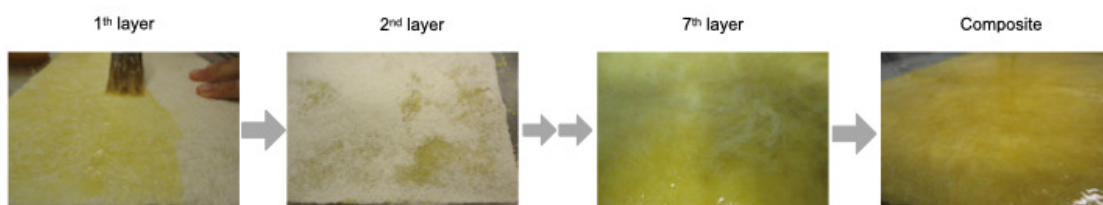


Figure 2: Representation of composites production steps

The wt% of the fiber mat was determined in a previous test. To produce this structure, thickness was

used as a parameter. Searching an answer to how much fiber could be used to produce a fiber mat with the

thickness between 3 and 4 mm, according to the process used to produce the mats, it was found that the answer corresponded to 6 and 10 wt% for these PU composites.

Accelerated weathering tests

Specimens of each sample (PU, T6, and T10) were identified and placed in the accelerated weathering chamber, following ASTM G154-00. The chamber was kept at (35.4 ± 1.4) °C, $(65.4 \pm 9.3)\%$ of RH and under UV radiation (80 W lamp and 1.4% UVA/UVB, *i.e.* a polychromatic emission spectrum in the range of UVB (290-320 nm) and UVA (320-400 nm)) for a photoperiod of 12 h. At predetermined times, as indicated before: 30, 60 and 90 days, specimens were randomly removed from the chamber and conditioned according to ASTM D618, as mentioned before.

Tensile and flexural tests

Test specimens were prepared from the composites for flexural tests according to ASTM D790-96, *i.e.* with the following dimensions: 127 mm in length, (12.7 ± 6.4) mm in width and (3.2 ± 0.4) mm in thickness. Similarly, according to ASTM 638-02a, the specimens for the tensile tests were cut to 165 mm in length, (19 ± 6.4) mm in width and (3.2 ± 0.4) mm in thickness. Before conducting these tests, the specimens were conditioned in agreement with the ASTM D618 packaging standard, *i.e.*, at the temperature of (23 ± 2) °C and relative humidity $(50 \pm 5)\%$ for 48 h.

Tensile and flexural tests were carried out according to ASTM 638-02a, with a strain rate of 5 mm min^{-1} , and ASTM D790-96, with a velocity of 2 mm min^{-1} , respectively, in an EMIC Universal Testing Machine model DL 10000/700, using a strain gouge to determine the modulus of elasticity. The results were reported as an average of at least five measurements, and the ANOVA was applied to the data, assuming the significance level of 5%. The asterisk (*) denotes statistically significant results, compared to the mean value of each sample achieved before aging.

Theoretical density and void content

In agreement with ASTM 2734 method A, the theoretical density and the void content were determined for T6 and T10 composites, applying Equation (1):

$$V (\%) = 100 (T_d - M_d) / T_d \quad (1)$$

where V = void content, volume %; T_d = theoretical composite density, and M_d = measured composite density (a mean of triplicate measurements).

RESULTS AND DISCUSSION

Table 1 shows the composition (hemicelluloses, lignin and cellulose), ash content, pH and density for PPF and PPF mats. For PPF, the hemicelluloses, lignin, and cellulose

percentages were 28.4, 8.9 and 54.4 wt%, respectively. These results agree with those identified in previous work on the same material.³³ Moreover, the cellulose percentage is similar to that found for Eucalyptus, the lignin content is reduced, being less than in sweet sorghum, while the hemicelluloses reach a similar percentage recorded for sugar bagasse.³⁴ Such a comparison with other common lignocellulose biomasses helps identify potential applications for the material investigated here.

The effect of acid hydroxide peroxide ($\text{H}_3\text{CCOOH-H}_2\text{O}_2$) dissociation of PPF on the relative contents of these components can be observed. The hemicelluloses and lignin decreased by 68% and 41% of the initial fiber value. While for cellulose, there was a relative increase of 39%, reaching 76%. This cellulose content of the microfibrils influences the material's performance, since reducing hemicelluloses after chemical treatment and the relative rise of cellulose in the fiber results in better mechanical properties, compared to untreated fiber.³⁵⁻³⁷

The ash content showed that more than 50% of the minerals were lost. This reduction in ash content during acid hydrolysis has been also reported in the literature.^{36,38} The fact that microfibrils extraction occurred in an acid medium may have contributed to the leaching of some minerals and may be responsible for reducing the pH from 6 to 4. The relative increase of cellulose resulted in a 55.6% increase in plant material density. The high cellulose content is directly related to the fracture toughness in plant materials, specifically the leaves.³⁷ Comparing with data reported in the literature, the contents of hemicelluloses, lignin, and cellulose of the peach palm fiber mats are similar to those of curauá (*Ananas erectifolius*) fibers.^{38,39} Due to its high cellulose content, curauá fiber has been recommended for application in composites, mainly in the automotive market³⁸ and, more recently, as one of the essential sources of nanocellulose for the production of nanocomposites.³⁹ Thus, the peach palm represents an alternative source to produce nanocellulose. The TG and DTG curves recorded the degradation temperature and the percentage of mass loss for each event, as summarized in Table 2, in comparison with the corresponding values for the fibers before dissociation (PPF).

Table 1
Composition (hemicelluloses, lignin and cellulose), ash content, pH, and density of peach palm fibers and fiber mat

| Plant material | Hemicellulose* | Lignin* | Cellulose* | Ashes* | pH | Density (kg.m ⁻³) |
|----------------|----------------|---------|------------|--------|-----|-------------------------------|
| PPF | 28.4 | 8.9 | 54.4 | 1.7 | 6.4 | 900 |
| Fiber mat | 9.1 | 5.3 | 75.9 | 0.6 | 4.3 | 1400 |

*dry mass percentage

Table 2
Data of degradation temperature and percentage of fiber mass loss before (PPF) and after dissociation (fiber mats), determined from TG/DTG curves

| Sample | 1° Stage | | 2° Stage | | 3° Stage | | | Residue (%) | |
|-----------|-------------------------|---------------------|-------------------------|-----------------------|---------------------|-------------------------|-----------------------|---------------------|----|
| | T _{onset} (°C) | Δm ₁ (%) | T _{onset} (°C) | T _{max} (°C) | Δm ₂ (%) | T _{onset} (°C) | T _{max} (°C) | Δm ₃ (%) | |
| PPF | 85 | 8.2 | 285 | 312 | 16.5 | 325 | 365 | 36.2 | 28 |
| Fiber mat | 72 | 8.3 | 325 | 352 | 75.4 | 375 | 458 | 6.5 | 10 |

The PPF presented three stages of mass loss, the first occurring around 85 °C, attributed to the evaporation of water. The second stage is attributed to hemicellulose depolymerization and the disruption of cellulose glycosidic bonds. A third stage partially overlapped with the second, presenting T_{onset} at 325 °C, was attributed to α-cellulose degradation, according to the literature for peach palm fibers.²⁷

Water evaporation occurs in the fiber mat at a lower temperature than in the PPF. Due to the small hemicelluloses content, this material does not show a degradation stage at 285 °C. At the same time, the events at T_{onset} = 325 °C and T_{onset} = 375 °C are attributed to cellulose degradation.⁴⁰ In agreement with the literature, the thermal degradation of cellulose involves dehydration, depolymerization, glycosyl-units decomposition, and charred residue formation.⁴¹

The percentage of cellulose-related mass loss recorded in the thermal analysis of the fiber mat is similar to that determined by physicochemical analysis and expressed in Table 1. In addition, the thermal stability of neat PU and the effect of the peach palm fiber mat on the TG and DTG curves of the composites, before (t0) and after 30 (t30), 60 (t60) and 90 (t90) days of accelerated weathering can be seen in Figure 3. The sample PU_t0 represents neat PU and allows identifying three stages of degradation: the first one, at T_{max} of 338 °C, related to the rupture of the urethane bonds, the second, at 383 °C, attributed to the split of ester bonds present in the prepolymer, and the third, at 478 °C, corresponding to polyol

degradation.^{30,42} For the composites, the three stages are also present, and the last two, considering the results of the pure components (PU and fiber mat), are events related to both the matrix and the filler.

Comparing the PU sample with the composites, it can be observed that both show almost the same thermal stability. Although sample T6 proves to be slightly more stable than the others. This improvement can be related to the dissociation process, since a chemical treatment increases the thermal stability of natural fiber polymer composites.⁴³⁻⁴⁷ On the other hand, the fiber mat percentage did not affect the residue mass differently, which is coherent, as at 325 °C the degradation of α-cellulose occurred. A negligible effect of fiber percentage in PU composites has been reported for *Luffa cylindrica*.⁴⁷

The effect of 90 days of accelerated weathering exposure on thermal stability is subtle. Another result of UV-accelerated weathering is that color changes (Fig. 4a) are more pronounced in neat PU samples than in the composites. The color change of aromatic PU exposed to UV-irradiation is well established, including the formation of quinone amide from the phenyl group. It can be correlated with photodegradation by a relative increase in the concentration of carbonyl groups.²⁹ Considering the di-isocyanate used in this study, the main mechanisms involved are mainly the photo-Fries and Norrish type I reactions,²⁹ the scission of the urethane group and oxidation of the central methylene group with

quinone (yellow) formation as a chromophoric reaction product as a layer on the polymer surface.^{30,42}

Concerning the mechanical tests, the samples did not show any sign of crack or rupture during the flexural assay. The same occurred with the

samples after all accelerated weathering periods. The NCO/OH ratio depends on isocyanate, and it confers more flexibility (ratio greater than 1) or more rigidity (lower than 1) to PU.^{48,49} The flexural test results agree with the properties of the PU resin used in this study.

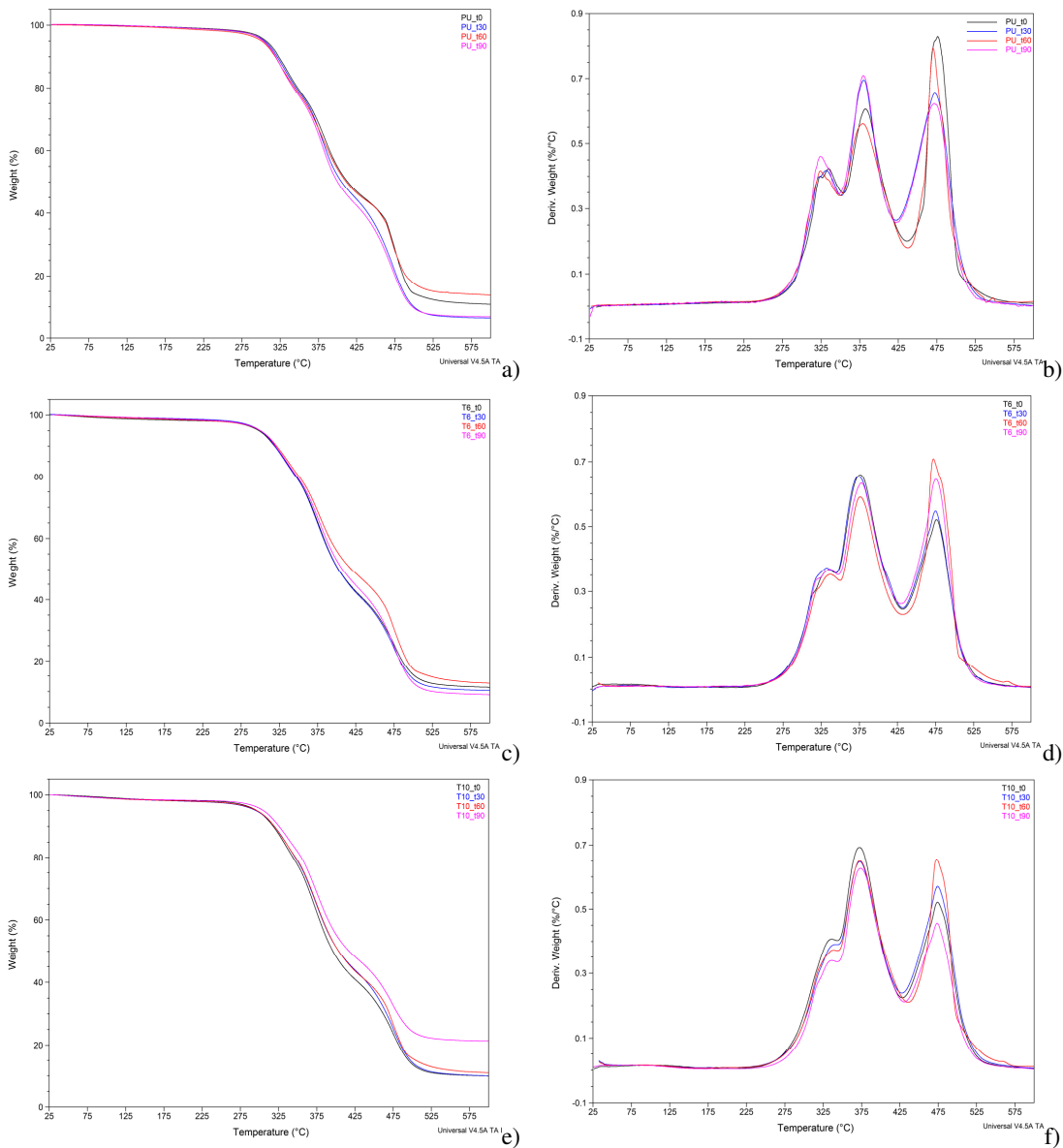


Figure 3: TG and DTG curves for PU (a and b), T6 (c and d) and T10 (e and f) samples before (t0) and after undergoing the accelerated weathering test for 30 (t30), 60 (t60) and 90 (t90) days

The results obtained in tensile tests and the effect of accelerated weathering on these properties are presented in Figure 4 (b, c and d). The PU_t0 sample presented a tensile strength of 11.5 MPa, a commonly recorded value for

thermoplastic polyurethane.⁵⁰ The statistical analysis signaled that after 60 days of UV-exposure, this sample's tensile strength was affected. After 90 days of exposure, a reduction of about 1.8 MPa in tensile strength occurred,

corresponding to a 15% loss in tensile performance attributed to the UV-degradation process.

The three samples before accelerated weathering demonstrate the effect of the fiber mat on composites' tensile strength, 6.5 MPa and 5.1 MPa for T6_t0 and T10_t0, respectively. Two factors contributed to this. One is the fiber mat that can interfere in the PU curing process. The other is related to the void content corresponding to 1.25% for PU, 4.37% for T6 and 6.35% for T10. It is known that the mechanical tests are

highly dependent on the porosity or integrity of the matrix, and the void content helps to identify a range of porosity that is associated with the manufacturing process.⁵¹ A standardization process for producing fiber mats can help reduce problems, such as porosity, which alter the mechanical results, as presented here. On the other hand, it was possible to observe that after 90 days, compared with t0, there was a reduction of 6.5% in tensile strength for T6 and a statistically insignificant decrease for the T10 sample.

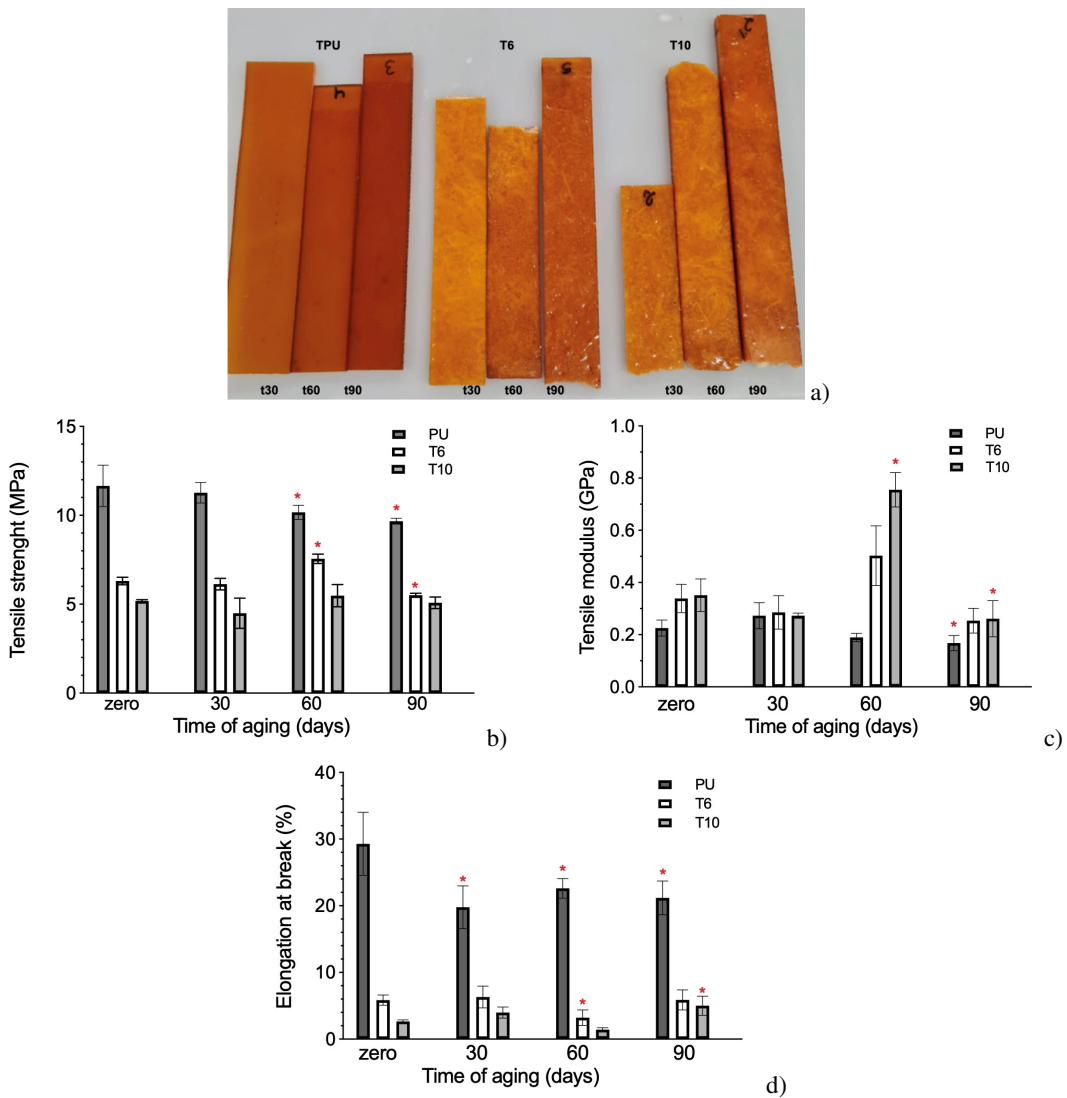


Figure 4: (a) Photograph of PU, T6 and T10 composites, (b) Tensile strength, (c) Modulus of elasticity and (d) Elongation at break for PU, T6 and T10 before (t0) and after 30, 60 and 90 days of UV aging
(*correspond to statistically different values ($p < 0.05$), compared to unaged samples)

Regarding the modulus of elasticity, the samples T6 and T10 at t0 (0.4 and 0.35 GPa) were significantly higher than that of PU (0.23 GPa). The increase in stiffness of the composites can be attributed to fiber incorporation,⁵⁰ mainly because fiber mats exhibit a random arrangement of fibrils (last image in Fig. 1), giving shape and some rigidity to this material. Weathering effects on these properties of the samples demonstrate that it is significantly impacted after 60 days of exposure, mainly T10 and PU, and T10 after 90 days. Neat PU slightly increased within 30 days, followed by a slight decrease after 90 days of exposure. While for composites, the fiber mat content showed a decrease within 30 days, T6 in 29% and T10 in 17%, followed by an evident stiffening effect at t60 (T6: 0.59 and T10: 0.78 GPa), followed by a decrease after 90 days reaching 0.26 GPa for both samples. In the literature, there is work suggesting that cellulose can stabilize UV-curable polymers.⁴⁹ Others report the use of di-isocyanates for crosslinking cellulose with the matrix. This kind of result is reached using different strategies,⁵² one of them being the introduction of cellulose directly, without modification, into the polyol/di-isocyanate mixture, which are then cured together. This crosslinking was accompanied by increased stability, enhancing the material strength. In short, the increase in tensile strength and modulus, for both composites, after 60 days of UV exposure, is coherent with the idea of crosslinking between cellulose from the surface of the fiber mat and di-isocyanate from the matrix. Not to mention that an extended UV-aging involves additional crosslinking to give a more

highly ordered structure and can be considered to explain the increase of Young's modulus of the UV-exposed polymers.⁵²

A reduction of the elongation at break because of increased fiber mat percentage was also evident at t0. Fiber incorporation led to significant decreases in elongation at break, 81 and 91% for T6 and T10, respectively.⁵³ Similarly, other authors⁵³ recorded a reduction in stretching for PU composites and sisal fibers. According to the accelerated weathering results, the elongation at break of the PU sample decreased by 32% after 30 days (t30), while the composites, independently of the fiber mat content, showed no statistically significant variation during the 90 days of exposure. The values determined in this study for the mechanical properties of Young's modulus and elongation at break of samples T6 and T10, at t0, are similar to those obtained for PU samples with cellulose nanocrystals (CNC) or with cellulose nanofibrils (CNF),⁵⁴ when considering PU/cellulose ratios close to those applied here. Two factors appear to affect tensile strength directly. One is the mode of incorporation of the cellulosic material in PU as a fiber mat. The other could be the dimensions of the fiber used in fiber mat production; while the homogeneous distribution of CNC or CNF contributes to increasing that resistance, the mats decreased it, suggesting that this structure (fiber mat) does not favor the incorporation of peach palm fibers in the PU matrix.

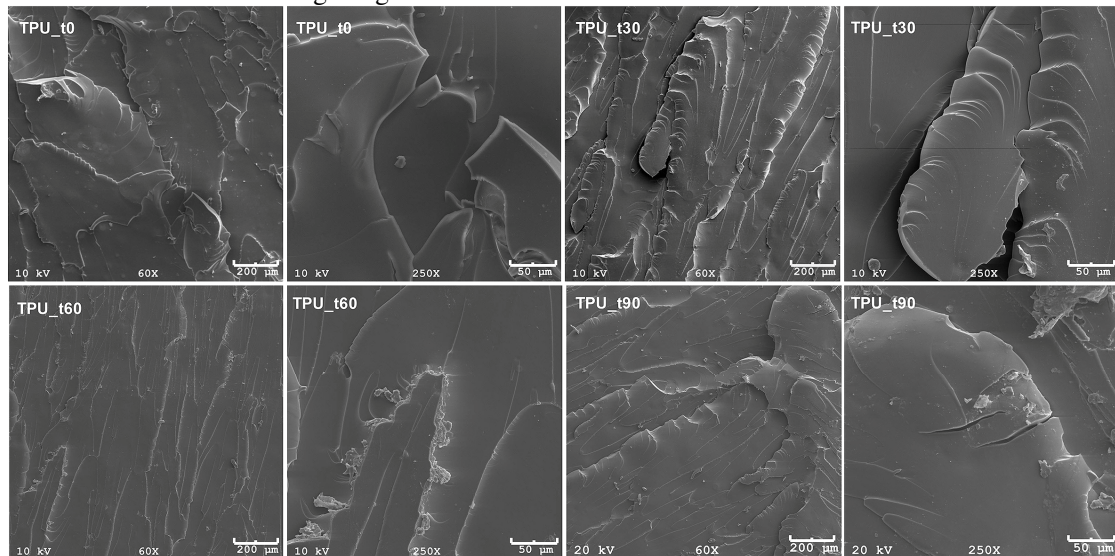


Figure 5: SEM micrographs of fracture surfaces of PU samples before and after different periods of exposure to accelerated weathering (60X and 250X magnification)

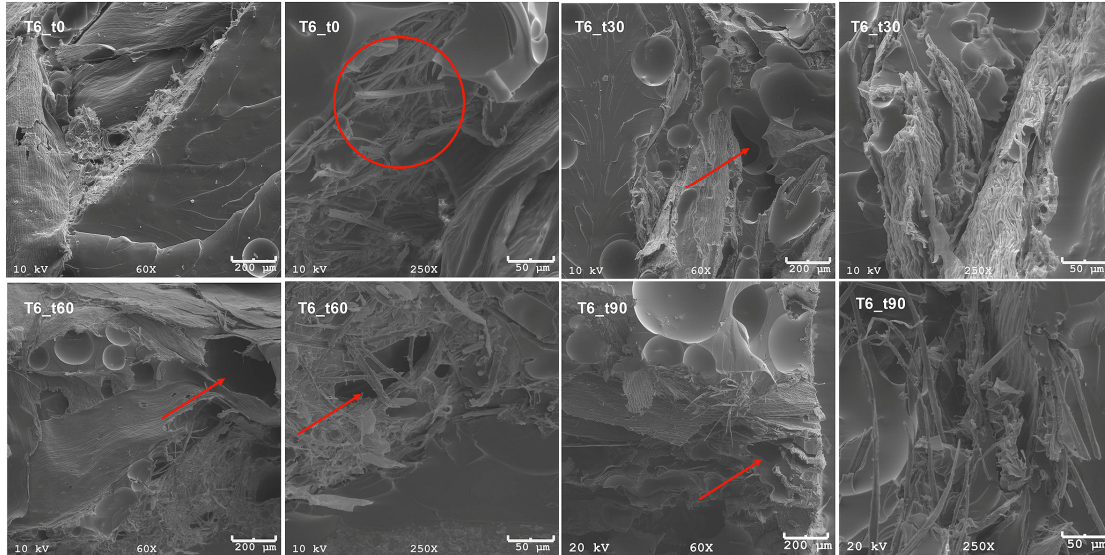


Figure 6: SEM micrographs of fracture surfaces of T6 samples before and after different periods of exposure to accelerated weathering (60X and 250X magnification)

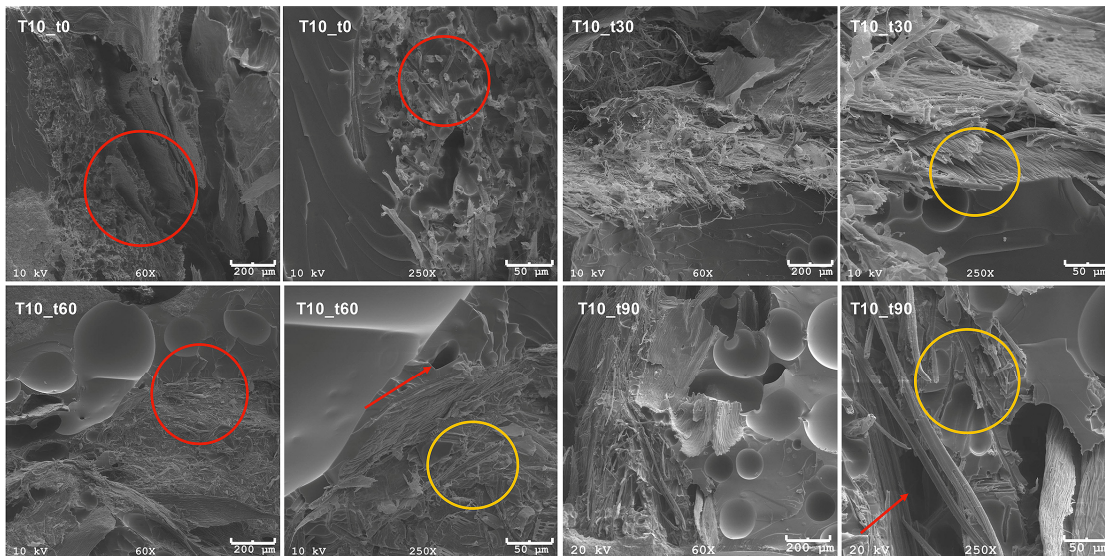


Figure 7: SEM micrographs of fracture surfaces of T10 samples before and after different periods of exposure to accelerated weathering (60X and 250X magnification)

As for dimensions of the fibers after the dissociation process, these presented a length around 1 mm,³¹ which represents a lower surface area available for interacting with the PU matrix.

Figure 5 shows the morphology of the PU fracture surfaces before (t0) and after 30 (t30), 60 (t60), and 90 (t90) days of weathering. The

micrograph of the fracture surface caused by the tensile test in PU_t0 denotes a fragile rupture, with scale-like chips, absence of bubbles, and smooth appearance. These aspects have not suffered noticeable changes over different aging test periods.

Concerning the T6 samples, shown in Figure 6, the fracture surface of T6_t0 showed the same type of fracture observed in the PU region as in the neat PU sample, and it is observable that the resin permeated the fibrils (red circle). In samples from T6_t30, it is possible to observe broken fibers (orange circles), indicating load transfer and some adhesion between fibers and matrix. Moreover, there are bubbles/voids (red arrows) in these samples, both in the matrix and in the fiber mat/matrix interface, which may have contributed to reducing the tensile strength of this composite, compared to the neat PU sample. Watching the micrograph set for the T10 samples (Fig. 7), the fractured image in T10_t0 is similar to that of the T6_t0 composite. However, the resin permeates the fibrils more heterogeneously, with smaller and more impregnated areas (red circles). It may be related to the mat's thickness, which is 0.1 mm higher than that for the 6wt% fiber mat. PU resin has more difficulty in diffusing through the fiber mat. In samples from T10_t30 and sample T6_t0, it is possible to observe ripped or smashed fibrils (orange circles) and the formation of bubbles/voids (red arrows) as well.

It can be seen that in the samples machined and exposed for 60 days in the chamber (T10_t60), the resin was well impregnated in the fiber mat, when compared to the samples subjected to other exposure periods. At the same time, it confirms the difficulty of impregnating the fiber mat homogeneously with the matrix. It is worth observing the formation of bubbles in the fracture region of the composites, an aspect absent in the PU samples. The most plausible hypothesis is that the air present in the fiber mat pores was displaced during curing, becoming trapped in the resin. It can be another factor that contributed to reducing the composites' tensile strength, compared to the PU sample.

CONCLUSION

Peach palm waste can be turned into fibrils composed of more than 75 wt% of cellulose. Such fibrils have been used to produce mats and, subsequently, by lamination, PU composites, with a random distribution of fibrils, and with 6 and 10 wt% of peach palm fiber content. The thermal stability of the composites was similar to that of neat PU samples, but the composites displayed lower tensile strength and elongation at break, and increased stiffness, compared to the matrix. SEM images showed the mats' impregnation by the matrix and the formation of bubbles. This set of

results can be, in part, explained by the manufacturing process of the composites, while fiber mats are considered suitable for this purpose due to the simplicity of the process. However, the low production control resulted in samples with many voids, which affected their mechanical performance. In addition, the impact of accelerated weathering was evident in the analyses of the mechanical results. Still, these mechanical results cast light on a different way of using the peach palm waste material, while the fiber mat production process can be improved and the fiber mat will be further tested with other polymers or for different applications.

ACKNOWLEDGMENTS: The authors thank the Univille Research Support Fund (FAP/Univille) for their financial support.

REFERENCES

- ¹ T. G. Y Yashas Gowda, M. R. Sanjay, K. S. Bhat, P. Madhu, P. Senthamaraiakannan *et al.*, *Cogent Eng.*, **5**, 1 (2018), <http://doi.org/10.1080/23311916.2018.1446667>
- ² Y. G. Thyavihalli Girijappa, S. Mavinkere Rangappa, J. Parameswaranpillai and S. Siengchin, *Frontier Mater.*, **6**, 226 (2019), <http://doi.org/10.3389/fmats.2019.00226>
- ³ T. Nishino, K. Hirao, M. Kotera, K. Nakamae and H. Inagaki, *Compos. Sci. Technol.*, **63**, 1281 (2003), [http://doi.org/10.1016/S0266-3538\(03\)00099-X](http://doi.org/10.1016/S0266-3538(03)00099-X)
- ⁴ H. Anuar and A. Zuraida, *Compos. Part B: Eng.*, **42**, 462 (2011), <http://doi.org/10.1016/j.compositesb.2010.12.013>
- ⁵ S. Kalia, B. S. Kaith and I. Kaur, *Polym. Eng. Sci.*, **49**, 1253 (2009)
- ⁶ M. R. Sanjay, G. R. Arpitha, L. L. Naik, K. Gopalakrishna and B. Yogesha, *Nat. Resour.*, **7**, 108 (2016), <http://doi.org/10.4236/nr.2016.73011>
- ⁷ M. Puttegowda, S. M. Rangappa, M. Jawaid, P. Shivanna, Y. Basavegowda *et al.*, in "Sustainable Composites for Aerospace Applications", edited by M. Jawaid and M. Thariq, Woodhead Publishing, 2018, pp. 315-351, <http://doi.org/10.1016/B978-0-08-102131-6.00021-9>
- ⁸ T. Väistönen, A. Haapala, R. Lappalainen and L. Tomppo, *Waste Manag.*, **54**, 62 (2016), <http://doi.org/10.1016/j.wasman.2016.04.037>
- ⁹ K. L. Pickering, M. G. A. Efendy and T. M. Le, *Compos.: Part A*, **83**, 98 (2016), <https://doi.org/10.1016/j.compositesa.2015.08.038>
- ¹⁰ G. R. Arpitha and B. Yogesha, *Mater. Today Proc.*, **4**, 2755 (2017), <http://doi.org/10.1016/j.matpr.2017.02.153>
- ¹¹ M. M. Kabir, H. Wang, K. T. Lau and F. Cardona, *Compos. Part B*, **43**, 2883 (2012), <http://dx.doi.org/10.1016/j.compositesb.2012.04.053>

- ¹² Z. Sydow and K. Bieńczak, *J. Nat. Fiber.*, **16**, 1189 (2018), <http://doi.org/10.1080/15440478.2018.1455621>
- ¹³ H. Kyutoku, N. Maeda, H. Sakamoto, H. Nishimura and K. Yamada, *Carbohyd. Polym.*, **203**, 95 (2019), <http://doi.org/10.1016/j.carbpol.2018.09.033>
- ¹⁴ A. K. Mohanty, S. Vivekanandhan, J.-M. Pin and M. Misra, *Science*, **362**, 536 (2018), <http://doi.org/10.1126/science.aat9072>
- ¹⁵ Y. Elmogahzy and R. Farag, in “Handbook of Properties of Textile and Technical Fibres”, edited by A. R. Bunsell, Woodhead Publishing, 2018, pp. 223-273, <http://doi.org/10.1016/B978-0-08-101272-7.00007-9>
- ¹⁶ H. Danso, *Proc. Eng.*, **200**, 1 (2017), <http://doi.org/10.1016j.proeng.2017.07.002>
- ¹⁷ A. O. Ogah and T. U. James, *Asian J. Phys. Chem. Sci.*, **5**, 1 (2018), <http://doi.org/10.9734/AJOPACS/2018/35841>
- ¹⁸ R. Arjmandi, A. Hassan and Z. Zakaria, in “Lignocellulosic Fibre and Biomass-Based Composite Materials”, edited by M. Jawaid, M. T. Paridah and N. Saba, Woodhead Publishing, 2017, pp. 77-94, <http://doi.org/10.1016/B978-0-08-100959-8.00005-6>
- ¹⁹ P. T. Anastas and J. C. Warner, “Green Chemistry: Theory and Practice”, New York, Oxford University Press, 1998, p. 60
- ²⁰ M. A. Farias, M. Z. Farina, A. P. T. Pezzin and D. A. K. Silva, *Mater. Sci. Eng. C*, **29**, 510 (2009), <http://doi.org/10.1016/j.msec.2008.09.02>
- ²¹ K. C. Batista, D. A. K. Silva, L. A. F. Coelho, S. H. Pezzin and A. P. T. Pezzin, *J. Polym. Environ.*, **18**, 346 (2010)
- ²² W. L. E. Magalhães, S. A. Pianaro, C. J. F. Granado and K. G. Satyanarayana, *J. Appl. Polym. Sci.*, **127**, 1285 (2013), <http://doi.org/10.1002/app.37633>
- ²³ C. Merlini, G. M. O. Barra, M. D. P. P. da Cunha, S. D. A. S. Ramôa, B. G. Soares *et al.*, *Polym. Compos.*, **38**, 2146 (2017), <http://doi.org/10.1002/pc.23790>
- ²⁴ J. S. P. da Silva, J. M. F. da Silva, B. G. Soares and S. Livi, *Compos. Part B: Eng.*, **129**, 117 (2017), <http://doi.org/10.1016/j.compositesb.2017.07.088>
- ²⁵ G. Soto, P. Luna-Orea, M. G. Wagster, T. J. Smyth and A. Alvarado, *Agron. J.*, **97**, 1396 (2005), <http://dx.doi.org/10.2134/agronj2004.0250>
- ²⁶ EMBRAPA Floresta, Transferência de Tecnologia Florestal: Pupunha, accessed on 14/10/21, <https://www.embrapa.br/florestas/transferencia-de-tecnologia/pupunha>
- ²⁷ C. Merlini, V. Soldi and G. M. O. Barra, *Polym. Testing*, **30**, 833 (2011), <http://doi.org/10.1016/j.polymertesting.2011.08.008>
- ²⁸ G. Oertel, “Polyurethane Handbook”, New York, Macmillan Publishing Co., Inc., 1985
- ²⁹ F. Xie, T. Zhang, P. Bryant, V. Kurusingal, J. M. Colwell *et al.*, *Progress Polym. Sci.*, **90**, 211 (2019), <https://doi.org/10.1016/j.progpolymsci.2018.12.003>
- ³⁰ D. Rosu, L. Rosu and C. N. Cascaval, *Polym. Degrad. Stabil.*, **94**, 591 (2009), <https://doi.org/10.1016/j.polymdegradstab.2009.01.013>
- ³¹ K. E. Quadros, S. Ghermann, M.Z. Farina, A.P.T. Pezzin and D.A.K. Silva, in *Procs. 60th National Congress of Botanics*, Feira de Santana, Brazil, 2009, p. 1
- ³² D. J. Silva, “Análise de alimentos: métodos químicos e biológicos” [Food Analysis: Chemical and Biological Methods], Viçosa, UFV, 1981
- ³³ M. F. L. B. Duprat, J. R. Rampinelli, S. G. de Lima, D. A. K. Silva, S. A. Furlan *et al.*, *Boletim do Centro de Pesquisa e Processamento de Alimentos*, **33**, 18 (2015)
- ³⁴ R. Kaur and P. Kaur, *Cellulose Chem. Technol.*, **55**, 207 (2021), <https://doi.org/10.35812/CelluloseChemTechnol.2021.55.21>
- ³⁵ K. O. Reddy, C. U. Maheswari, M. Shukla and A. V. Rajulu, *Mater. Lett.*, **67**, 35 (2012), <https://doi.org/10.1016/j.matlet.2011.09.027>
- ³⁶ A. M. Adel, Z. H. A. El-Wahab, A. A. Abraham and M. T. Al-Shemy, *Biore sour. Technol.*, **101**, 4446 (2010), <https://doi.org/10.1016/j.biortech.2010.01.047>
- ³⁷ K. Kitajima, S. J. Wright and J. W. Westbrook, *Interface Focus*, **6**, 20150100 (2016), <https://doi.org/10.1098/rsfs.2015.0100>
- ³⁸ P. A. Santos, M. A. Spinacé, K. G. Fermoselli and M. A. de Paoli, *Polímeros*, **19**, 31 (2009)
- ³⁹ S. F. Souza, M. Ferreira, M. Sain, M. Z. Ferreira, H. F. Pupo *et al.*, in “Biofiber Reinforcements in Composite Materials”, edited by O. Faruk and M. Sain, Elsevier, 2015, pp. 700-720
- ⁴⁰ G. A. Bernabé, M. Kobelnik, S. Almeida, C. A. Ribeiro and M. S. Crespi, *J. Therm. Anal. Calorim.*, **111**, 589 (2013), <https://doi.org/10.1007/s10973-012-2276-8>
- ⁴¹ A. Kumar, Y. S. Negi, V. Choudhary and N. K. Bhardwaj, *J. Mater. Phys. Chem.*, **2**, 1 (2014), <http://pubs.sciepub.com/jmpc/2/1/1DOI:10.12691/jmpc-2-1-1>
- ⁴² A. Boubakri, N. Guermazi, K. Elleuch and H. F. Ayedi, *Mater. Sci. Eng. A*, **527**, 1649 (2010), <https://doi.org/10.1016/j.msea.2010.01.014>
- ⁴³ B. Singh, M. Gupta and A. Verma, *Polym. Compos.*, **17**, 910 (1996), <https://doi.org/10.1002/pc.10684>
- ⁴⁴ Y. Xie, C. A. S. Hill, Z. Xiao, H. Militz and C. Mai, *Compos. Part A*, **41**, 806 (2010), <https://doi.org/10.1016/j.compositesa.2010.03.005>
- ⁴⁵ Y. Xu, J. Salmi, E. Kloster, F. Perrin, S. Grosse *et al.*, *Ind. Crop. Prod.*, **51**, 381 (2013), <https://doi.org/10.1016/j.indcrop.2013.09.029>
- ⁴⁶ Y. Chen, N. Su, K. Zhang, S. Zhu, Z. Zhu *et al.*, *Ind. Crop. Prod.*, **123**, 341 (2018), <https://doi.org/10.1016/j.indcrop.2018.06.079>
- ⁴⁷ B. N. Melo, V. M. D. Pasa, M. D. M. Martins, W. A. A. Macedo and E. P. Muniz, *J. Polym. Environ.*, **26**,

- 2514 (2018), <https://doi.org/10.1007/s10924-017-1148-5>
- ⁴⁸ R. Gogoi, M. S. Alan and R. K. Khandal, *Int. J. Basic Appl. Sci.*, **3**, 118 (2014), <https://doi.org/10.14419/ijbas.v3i2.2416>
- ⁴⁹ M. Hubmann, X. Kong and J. M. Curtis, *Progress Org. Coat.*, **129**, 101 (2019), <https://doi.org/10.1016/J.PORGCOAT.2018.12.019>
- ⁵⁰ A. A. Mohammed, D. Bachtiara, M. R. M. Rejaba, S. F. Hasany and J. P. Siregar, *Theor. Found. Chem. Eng.*, **53**, 454 (2019), <https://doi.org/10.1134/S0040579519030072>
- ⁵¹ D. Saenz-Castillo, M. I. Martín, S. Calvo, F. Rodriguez-Lence and A. Güemes, *Compos. Part A*, **121**, 308 (2019), <https://doi.org/10.1016/j.compositesa.2019.03.035>
- ⁵² H. Abushammala and J. Mao, *Molecules*, **24**, 2782 (2019), <https://doi.org/10.3390/molecules24152782>
- ⁵³ E. Głowińska, J. Datta and P. Parcheta, *J. Therm. Anal. Calorim.*, **3**, 113 (2017), <https://doi.org/10.1007/s10973-017-6293-5>
- ⁵⁴ K. Benhamou, H. Kaddami, A. Magnin, A. Dufresne and A. Ahmad, *Carbohydr. Polym.*, **122**, 202 (2015), <http://dx.doi.org/10.1016/j.carbpol.2014.12.081>